ELSEVIER

22 April 1996

PHYSICS LETTERS A

Physics Letters A 213 (1996) 155–166

Multiplexing chaotic signals using synchronization

Lev S. Tsimring [a], Mikhail M. Sushchik [a,b]

[a] *Institute for Nonlinear Science, University of California, San Diego, La Jolla, CA 92093-0402, USA*

[b] *Department of Physics, University of California, San Diego, La Jolla, CA 92093-0354, USA*

Received 29 September 1995; revised manuscript received 12 January 1996; accepted for publication 31 January 1996
Communicated by A.R. Bishop

Abstract

Chaotic synchronization usually involves two coupled chaotic systems, with either one driving the other, or both being mutually coupled. In this paper we address a problem of synchronizing more than one pair of chaotic systems using only one communication channel. We demonstrate the principal possibility of multiplexing chaotic signals using synchronization both for iterated maps and ordinary differential equations. Possible applications for communication purposes are discussed.

Keywords: Chaotic synchronization; Multiplexing; Coupled maps; Intermittency

1. Introduction

In the last decade, the phenomenon of synchronous chaotic behavior in coupled nonlinear systems has been studied in much detail both theoretically and experimentally (see e.g. Refs. [1,2]). There are two settings in which chaotic synchronization is most commonly considered. In the first one a uni-directional coupling is introduced between a driving chaotic system and the response system which can either be identical to it or replicate a sub-system of the driving system. In the second more general approach, a mutual coupling between two systems leads to their synchronization. In both cases, the regime of identical synchronization when the corresponding variables in two coupled systems exhibit identical chaotic oscillations, can often be achieved by using a scalar variable for coupling, in other words, one "communication channel" between the two systems is usually enough.

Recently it has been proposed to use nonlinear chaotic oscillators for communication. A chaotic system can be controlled by small external perturbations in such a way as to produce a given symbolic sequence [3]. Alternatively, a small-magnitude message can be added to a chaotic signal and then recovered at the receiver end, thereby providing a private communication link [4].

For linear systems, there are a number of standard ways to increase the information capacity of the channel by sending multiple signals over one channel. Most common are frequency division and time multiplexing [5]. More recently, various spread-spectrum methods of channel multiplexing based on digital signal processing were introduced for communication purposes [6]. Many of these schemes involve random or pseudo-random masking of the digital signal. Uncoupled chaotic systems generate uncorrelated signals which can be used for

PII S0375-9601(96)00118-1

information transmission. It would be of great interest to exploit intrinsic properties of chaotic systems for signal multiplexing and spread-spectrum communication.

In this paper, we address the issue of multiplexing chaotic signals using synchronization. By that we mean the ability to identically synchronize several pairs of chaotic oscillators using just one communication link. The signal transmitted through this link represents a combination (in the simplest case considered here, a linear superposition) of the scalar signals from the driving oscillators. In the synchronous regime the corresponding driving and response systems exhibit identical chaotic oscillations. Thus, when this regime is stable, one in fact is able to separate the composite transmitted signal onto several chaotic components which were produced by independent driving chaotic systems. We will show that stable synchronization is indeed possible with a particular choice of systems and a form of coupling.

In Section 2, synchronization of discrete-time systems (maps) is considered. In Subsection 2.1 we discuss the case of two system pairs, and in Subsection 2.2, a general case of N system pairs. The basin of attraction of synchronized dynamics shrinks as the number of pairs increases, and the system gets more and more sensitive to noise: bursts of de-synchronizations interrupt "laminar" phases of synchronized dynamics. Subsection 2.3 is devoted to a detailed analysis of the intermittent breaking of multiple synchronization due to additive noise in a communication channel. Section 3 deals with continuous-time systems of ODEs.

2. Discrete systems

2.1. Two system pairs

We begin our discussion with a simple model of two pairs of one-dimensional chaotic maps in the form

$$x_1(n+1) = f_1(x_1(n)), \tag{1}$$

$$x_2(n+1) = f_2(x_2(n)), \tag{2}$$

$$y_1(n+1) = f_1(y_1(n)) + \epsilon\left[f_1(x_1(n)) + f_2(x_2(n)) - f_1(y_1(n)) - f_2(y_2(n))\right], \tag{3}$$

$$y_2(n+1) = f_2(y_2(n)) + \epsilon\left[f_1(x_1(n)) + f_2(x_2(n)) - f_1(y_1(n)) - f_2(y_2(n))\right]. \tag{4}$$

Eqs. (1), (2) represent two different uncoupled driving systems, and (3), (4) are the respective response systems. Functions $f_{1,2}$ describe individual dynamics of maps[1], and ϵ denotes the strength of dissipative coupling. As one can see, in this case both response systems receive the same signal from the driving maps, $f_1(x_1(n)) + f_2(x_2(n))$, and therefore it can be transmitted through a single link. Note that unlike the driving maps, the response systems are coupled to each other. It is easy to see that the synchronized dynamics of both pairs of systems, $x_1(n) = y_1(n)$ and $x_2(n) = y_2(n)$, is an invariant manifold of the joint system (1)–(4). The main question is to see if this manifold can be made stable. Linear stability of the synchronization manifold is determined by the conditional Lyapunov multipliers (or exponents, see Ref. [2]). These, due to ergodicity, can be computed as the eigenvalues of the Oseledec matrix [7]:

$$\mathrm{OSL} = \lim_{N\to\infty}\left\{\mathrm{DF}^N(\boldsymbol{x})\cdot\left[\mathrm{DF}^N(\boldsymbol{x})\right]^T\right\}^{1/2N}, \tag{5}$$

where we have defined the matrix $\mathrm{DF}^N(\boldsymbol{x}(n))$ as the product of the conditional Jacobian matrices:

$$\mathrm{DF}^N(\boldsymbol{x}(n)) \equiv \prod_{i=0}^{N-1}\mathrm{DF}(\boldsymbol{x}(n+i)). \tag{6}$$

[1] We assume identical dynamics of corresponding driving and response systems throughout the paper.

For the oscillations in the synchronization manifold $x_{1,2}(n) = y_{1,2}(n)$, the Jacobian matrix for the response systems (3), (4) is given by

$$\mathrm{DF} = \begin{pmatrix} (1-\epsilon) f_1'(x_1(n)) & -\epsilon f_2'(x_2(n)) \\ -\epsilon f_1'(x_1(n)) & (1-\epsilon) f_2'(x_2(n)) \end{pmatrix}, \tag{7}$$

and is in general a function of the vector of variables $\boldsymbol{x}(n) = \{x_1(n), x_2(n)\}$ (the prime in (7) means differentiation with respect to an argument). We shall call this matrix the *conditional* Jacobian matrix. Since for arbitrary maps, elements of the conditional Jacobian DF are functions of x_1, x_2, it is impossible to calculate eigenvalues of the Oseledec matrix in a general form. However, a significant simplification is achieved for the value of $\epsilon = 1/2$ (in this case Jacobians become singular). Indeed, in this case, direct calculation yields

$$\mathrm{DF}^N(\boldsymbol{x}(n)) = 2^{-N} \prod_{i=0}^{N-1} \left[f_1'(x_1(n+i)) + f_2'(x_2(n+i)) \right] \begin{pmatrix} 1 & -1 \\ -1 & 1 \end{pmatrix}, \tag{8}$$

so two eigenvalues of the Oseledec matrix, also known as the conditional Lyapunov multipliers (their logarithms are conditional Lyapunov exponents [2]), in this case are

$$\lambda_1 = 0, \tag{9}$$

$$\lambda_2 = \frac{1}{2} \lim_{N\to\infty} \left(\prod_{i=0}^{N-1} \left[f_1'(x_1(n+i)) + f_2'(x_2(n+i)) \right]^2 \right)^{1/2N}. \tag{10}$$

Thus, for the linear stability of the invariant manifold of synchronized oscillations, a magnitude of the geometrical average of the sum of derivatives $f_1'(x_1(n)) + f_2'(x_2(n))$ must be less than 2. It can be achieved in the case of chaotic maps if at least some multipliers in the above product of the sum of derivatives are small enough. In fact, this is the case for many typical mappings.

Let us take an example of tent maps,

$$f_1(x) = ax, \qquad \text{if } x < 0.5,$$
$$= a(1-x), \qquad \text{if } x > 0.5, \tag{11}$$
$$f_2(x) = bx, \qquad \text{if } x < 0.5,$$
$$= b(1-x), \qquad \text{if } x > 0.5, \tag{12}$$

and $1 < \{a, b\} < 2$. If a is close to b, the sum $f_1'(x_1(n)) + f_2'(x_2(n))$ will be small when $x_1(n) < 0.5$ and $x_2(n) > 0.5$ or vice versa. Denote by p_1 (p_2) the probability for $x_1 < 0.5$ ($x_2 < 0.5$), and $q_{1,2} = 1 - p_{1,2}$. Then, due to the ergodicity,

$$\lambda_2 = \tfrac{1}{2}(a+b)^{p_1p_2+q_1q_2} |a-b|^{p_1q_2+q_1p_2}. \tag{13}$$

Clearly, for $|a-b| \to 0$, $\lambda_2 \to 0$. The two-dimensional plot of $\lambda_2(a,b)$ for two tent maps is shown in Fig. 1a. One can see that linear stability ($\lambda_2 < 1$) is achieved in the wide range of map parameters. It is interesting to note that for two shift maps,

$$f_1(x) = ax \bmod 1,$$
$$f_2(x) = 1 - bx \bmod 1, \tag{14}$$

when $|a-b| \to 0$, the eigenvalue λ_2 turns into zero even faster, as *all* multipliers in the product (10) are close to zero.

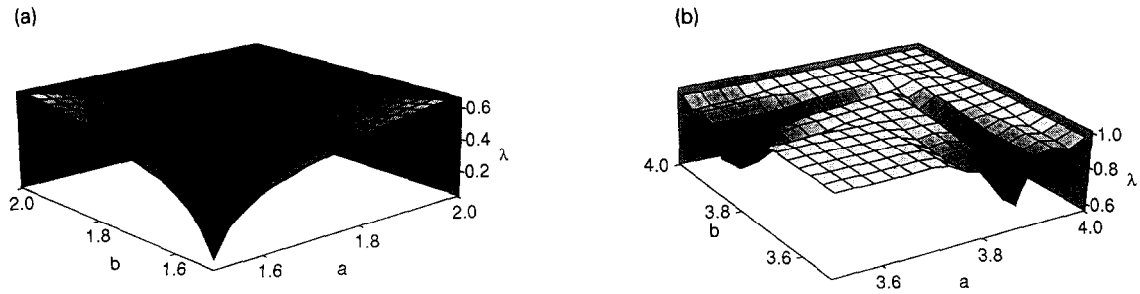

Fig. 1. Conditional multiplier for two pairs of coupled tent maps (a) and logistic maps (b) as a function of parameters a and b.

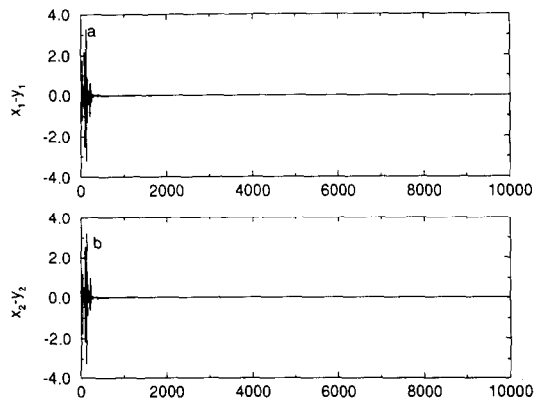

Fig. 2. Differences between driving and response signals $x_1 - y_1$ (a) and $x_2 - y_2$ (b) for two pairs of coupled logistic maps with parameters $a = 3.7$, $b = 3.8$, and coupling $\epsilon = 0.5$.

In the case of two logistic maps,

$$f_1(x_1) = ax_1(1 - x_1), \tag{15}$$

$$f_2(x_2) = bx_2(1 - x_2), \tag{16}$$

the Jacobians for individual maps fluctuate chaotically. Still, λ does not exceed 1 throughout the whole range of parameters a, b corresponding to chaotic dynamics of individual mappings (see Fig. 1b). These results suggest that synchronization of two pairs of maps is indeed possible. Fig. 2 demonstrates this synchronization in numerical experiments with two coupled pairs of logistic maps, with parameters $a = 3.7$ and $b = 3.8$, started from random initial conditions. The time series of y_1 eventually approaches that of x_1 while $y_2 \to x_2$. Similar behavior is observed for coupled tent maps.

2.2. *N system pairs*

Can one generalize this example and provide synchronization for more than two pairs of maps? The answer is "yes", however it requires a specific choice of maps. We will see that stable synchronization can be achieved in a particular class of complex mappings (i.e. a complex signal, or two scalar signals must be transmitted over a communication link).

Consider a collection of maps coupled again via a sum of the variables

$$x_j(n+1) = f_j\left(x_j(n)\right), \tag{17}$$

$$y_j(n+1) = f_j\left(y_j(n)\right) + \epsilon \sum_{i=1}^{N} \left[f_j\left(x_j(n)\right) - f_j\left(y_j(n)\right)\right], \qquad j = 1, \ldots, N. \tag{18}$$

The conditional Jacobian matrix for the response system reads

$$\mathrm{DF} = \begin{pmatrix} (1-\epsilon) f_1'(x_1(n)) & -\epsilon f_2'(x_2(n)) & \cdots & -\epsilon f_N'(x_N(n)) \\ -\epsilon f_1'(x_1(n)) & (1-\epsilon) f_2'(x_2(n)) & \cdots & -\epsilon f_N'(x_N(n)) \\ \vdots & \vdots & & \vdots \\ -\epsilon f_1'(x_1(n)) & -\epsilon f_2'(x_2(n)) & \cdots & (1-\epsilon) f_N'(x_N(n)) \end{pmatrix}. \tag{19}$$

To investigate the stability of the synchronization manifold of systems (17), (18) we shall begin with the analysis of the eigenvalues of this matrix. Let us make a simplification by assuming that all $f_j' = \text{const}$ for any $x_j(n)$ (as in shift maps). Thus we have a constant matrix

$$\mathrm{DF} = \epsilon \begin{pmatrix} (\epsilon^{-1}-1) f_1' & -f_2' & \cdots & -f_N' \\ -f_1' & (\epsilon^{-1}-1) f_2' & \cdots & -f_N' \\ \vdots & \vdots & & \vdots \\ -f_1' & -f_2' & \cdots & (\epsilon^{-1}-1) f_N' \end{pmatrix}. \tag{20}$$

A well-known theorem of the matrix theory [10] states that the characteristic equation of a matrix has the following general form:

$$\lambda^N + g_{N-1}\lambda^{N-1} + \ldots + g_1\lambda + g_0 = 0, \tag{21}$$

Here g_{N-r} is $(-1)^r$ times a sum of all main minors of the rth order of the matrix DF. It is easy to observe that for DF (20) the sum of all main minors of the rth order is proportional to the elementary symmetrical polynomial of the rth order, namely,

$$\begin{aligned} &g_{N-1} = -\det \mathsf{A}_1 (f_1' + f_2' + \ldots + f_N'), \qquad g_{N-2} = \det \mathsf{A}_2 (f_1' f_2' + f_1' f_3' + \ldots), \qquad \ldots, \\ &g_{N-r} = (-1)^r \det \mathsf{A}_r \sum_{i=1}^{C_N^r} f_{i_1}' f_{i_2}' \cdots f_{i_r}', \qquad \ldots, \qquad g_0 = (-1)^N \det \mathsf{A}_N f_1' f_2' \cdots f_N', \end{aligned} \tag{22}$$

where A_r is an $r \times r$ matrix of the following form:

$$\mathsf{A}_r = \begin{pmatrix} \epsilon^{-1}-1 & -1 & \cdots & -1 \\ -1 & \epsilon^{-1}-1 & \cdots & -1 \\ \vdots & \vdots & & \vdots \\ -1 & -1 & \cdots & \epsilon^{-1}-1 \end{pmatrix}. \tag{23}$$

First of all, notice that $\det \mathsf{A}_N = 0$ for $\epsilon = 1/N$. It turns out that one can make all $g_1, \ldots, g_{N-1} = 0$ by a particular choice of f_j'. Indeed, if f_j' are the roots of a polynomial of the Nth order,

$$f'^N + c_{N-1} f'^{N-1} + \ldots + c_1 f' + c_0 = 0, \tag{24}$$

from a well-known relationship between the roots of a polynomial and its coefficients, c_i must be equal to $g_i / \det \mathsf{A}_i$ (see (22)). Since we require all $g_1, \ldots, g_{N-1} = 0$, Eq. (24) reduces to a very simple form,

$$f'^N + c_0 = 0, \tag{25}$$

where c_0 is arbitrary. Evidently, the roots of this equation for $N > 2$ are complex,

$$f'_r = f_0 e^{2\pi i r/N}, \tag{26}$$

where f_0 is a new arbitrary complex constant. Since $g_1, \ldots, g_{N-1} = 0$ for this choice of f'_r and $\epsilon = 1/N$, the eigenvalues of DF (19) are all zero. It is known from the matrix theory [10] that matrices of this type are *nilpotent*, i.e. their finite power $\mathrm{DF}^n = \mathbf{0}$ for any $n \geqslant n_0$, where $n_0 \leqslant N$ (in fact, in this case $n_0 \equiv N$). The conditional Jacobians describe the evolution of small perturbations $\boldsymbol{\xi}(n) \equiv \boldsymbol{x}(n) - \boldsymbol{y}(n)$ transversal to the synchronization manifold. A jth iteration of $\boldsymbol{\xi}(n)$, $\boldsymbol{\xi}(n+j)$, is given by $\mathrm{DF}^j \boldsymbol{\xi}(n)$. Therefore, an arbitrary small perturbation off the inertial manifold $x_j = y_j$ will turn into zero within a finite number of iterations of the maps (17), (18), and so the synchronized dynamics is super-stable. The solution which we found implements the stable synchronization for *complex* maps, and therefore, *two* scalar variables, the real and imaginary part of the sum of dynamical variables need to be transmitted in order to synchronize more than two pairs of maps. In order to make the maps expanding, we must choose $f_0 > 1$, and to make the dynamic bounded we should take $f_j(x) = f'_j x \pmod 1$, which for complex maps means

$$f_j(x) = \left[\mathrm{Re}\left(f'_j x\right) \pmod 1\right] + \mathrm{i}\left[\mathrm{Im}\left(f'_j x\right) \pmod 1\right]. \tag{27}$$

Thus we established the principal possibility of multiplexing chaotic signals using synchronization. In the synchronized state the array of globally coupled response maps serves as the signal processing machine which takes the sum of chaotic sequences as its input and breaks it into the individual chaotic components each of which comes from a particular driving map.

We tested the synchronization of multiple maps with individual dynamics described by (27) in numerical simulations. If the system is started from the close neighborhood of the synchronization manifold $x_j = y_j$, it synchronizes quickly and remains synchronous for a long time. However, we found that the basin of attraction for the synchronous state shrinks rapidly as the number of maps increases. It turns out that the roundoff errors eventually may lead to de-synchronization. This effect depends strongly on the number of coupled maps. For example, when double precision is used, one can synchronize up to $N = 43$ pairs of maps for over 10000 iterations. With single precision, only up to $N = 13$ pairs could be synchronized over the same number of iterations. In the next subsection we will explore the role of noise in greater detail.

2.3. *Noise in the channel*

It is known that even a small amount of noise, either in the communication channel, or in the systems themselves (for example a small mismatch of the parameters in the corresponding systems), affects the synchronization quite adversely [11]. The same is true for the synchronization of periodic oscillations in large arrays of globally coupled oscillators [12]. The basins of attraction of synchronized states shrink rapidly with the number of elements in the array and arbitrarily small noise is able to destroy synchronization. We observe the similar phenomenon in the synchronization of many pairs of chaotic systems coupled via one communication channel when the channel introduces small fluctuations into the driving signal.

In Fig. 3 we show the difference $x_1 - y_1$ for two pairs of coupled tent maps ($a = 1.8$, $b = 1.9$) when the same white noise uniformly distributed between $-\sigma/2$ and $\sigma/2$ is added to all the r.h.s. of response maps (this simulates an additive noise in the communication channel). Perhaps not surprisingly, the difference exhibits a clear intermittent behavior. Indeed, there is a very close similarity between this phenomenon and so-called "on–off" intermittency [8]. As in the latter case, even when the system is under the threshold of intermittency for the noise-free case, very small amounts of noise yield intermittent burstings. The underlying reason for this "below-threshold" intermittency is the presence of *local* conditional multipliers with magnitude greater than 1. The local conditional multiplier for a system (1)–(4) with $\epsilon = 1/2$ is determined as the eigenvalue of the finite product of Jacobians,

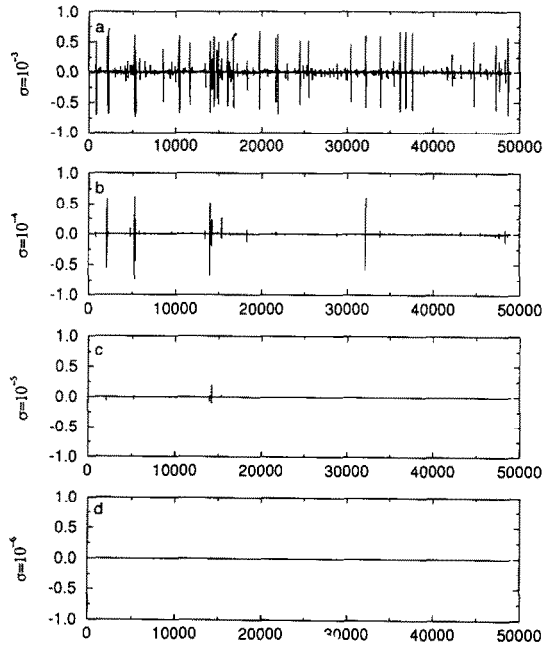

Fig. 3. Differences between driving and response signals $x_1 - y_1$ for two pairs of coupled tent maps with parameters $a = 1.8$, $b = 1.9$, and coupling $\epsilon = 0.5$, when white noise is added to the synchronizing signal, for various noise levels σ.

$$\lambda(N; x_1(n), x_2(n)) = \frac{1}{2}\left(\prod_{i=0}^{N-1}\left[f_1'(x_1(n+i)) + f_2'(x_2(n+i))\right]^2\right)^{1/2N}, \tag{28}$$

so there is a finite probability to find $\lambda(N) > 1$. One can introduce a measure of local instability as

$$\Lambda_{\max}(x_1, x_2) = \sup_N \left[\lambda(N; x_1, x_2)\right]^N. \tag{29}$$

When $\Lambda_{\max}$ reaches a value which is of the order of σ^{-1}, a small $O(\sigma)$ initial fluctuation of $|x(n) - y(n)|$ due to noise in the channel may grow to $O(\Lambda_{\max}\sigma) = O(1)$ after several iterations, and the system can escape from the linear neighborhood of the inertial manifold and produce a burst of de-synchronized behavior. In particular, for the case of coupled tent maps with $a \simeq b$, these "susceptible" intervals happen when $G \equiv f_1'(x_1(n)) \cdot f_2'(x_2(n)) > 0$, for many consecutive iterations. In this case $\Lambda_{\max} \simeq |a|^N$, where N is the number of consecutive iterations with $G > 0$ starting with a given iteration n. Fig. 4 illustrates this point: in Fig. 4a the deviation $|x_1 - y_1|$ is shown for each iteration n and in Fig. 4b $\Lambda_{\max}$ is plotted for the same run. Of course, not every interval with high $\Lambda_{\max}$ necessarily produces a burst of de-synchronization, but still a strong correlation between peaks of $\Lambda_{\max}$ and intermittent bursts of de-synchronization is clearly seen in the figure.

In the case of shift maps (14), all local multipliers are formally zero if they are computed for segments of lengths equal or larger than the number of driving maps. However, in this case, when some small noise is transmitted together with the driving signal, synchronization also breaks down after a while. The synchronization breakdown occurs when one of the driving maps produces a signal which is very close to the shift value ($\mathrm{Re}\,|x_j - 1| < O(\sigma)$ or $\mathrm{Im}\,|x_j - 1| < O(\sigma)$). In this case, the noise in the communication channel may force one of the response maps to shift while the corresponding driving map did not shift, or vice versa. This causes the coupling terms in all response maps to deviate from zero significantly which destroys the synchronization

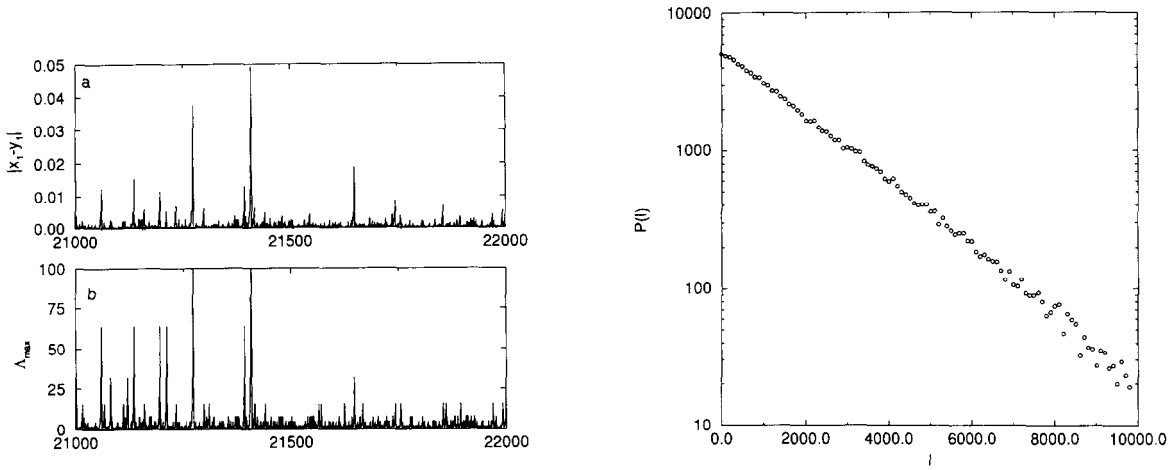

Fig. 4. (a) Magnitude of the difference between driving and response signals $|x_1 - y_1|$ for two pairs of coupled tent maps with parameters $a = 1.8$, $b = 1.9$, $\epsilon = 0.5$, and $\sigma = 10^{-3}$; (b) simultaneous time series of Λ_{max}.

Fig. 5. An example of the probability distribution of lengths of laminar phases for coupled complex shift maps (14) with $f_0 = 1.5, \epsilon = 0.333$ and $N = 3$, $\sigma = 2 \times 10^{-4}$. For other values of N and σ distributions $P(l)$ are qualitatively similar.

in the whole system. Since for large N the basin of attraction of the synchronous state is small, the system can spend a very long time before returning to a synchronous state again.

We analyzed the statistics of the lengths of synchronous periods for various numbers of maps N and noise levels σ. The results are presented in Figs. 5–8. It turns out that the distribution function of "laminar phases" $P(l)$ obeys an exponential law,

$$P(l) \propto \mathrm{e}^{-\Delta l}, \tag{30}$$

with the rate Δ depending on N and σ (see Fig. 5). It is easy to explain the exponential statistic (30). Indeed, as mentioned above, the synchronous phase ends when one of the variables x_j and its counterpart y_j happen to be on opposite sides of the shifting boundary. Therefore, $P(l_0)$ is the probability that this does not occur at any $l < l_0$ and occurs at $l = l_0$. What is the probability $P_R(j)$ that at the step l $\mathrm{Re}\, f_j' x_j < 1$ and $\mathrm{Re}\, f_j' y_j > 1$? Evidently, it can be expressed by an integral

$$P_R(j) = \int_0^1 \int_{1-\tau}^{\infty} \Pi_j(\tau) G_j(\nu)\, \mathrm{d}\tau\, \mathrm{d}\nu, \tag{31}$$

where $\Pi_j(\tau)$ is the probability distribution for $\mathrm{Re}\, x_j$ and $G_j(\nu)$ is the probability distribution for $\mathrm{Re}(x_j - y_j)$. Shift maps themselves produce uniform distributions for the variables x_j within the squares $0 < \mathrm{Re}\, x_j < 1$, $0 < \mathrm{Im}\, x_j < 1$ (small noise does not change it significantly), so the probability $\Pi_j(\tau) = 1$. Assuming that $G_j(\nu)$ has a Gaussian distribution (this assumption is reasonable in virtue of the Central Limit theorem),

$$G_j(\nu) = \frac{1}{\sqrt{\pi}\sigma_R(j)} \mathrm{e}^{-\nu^2/\sigma_R(j)^2}, \tag{32}$$

one can readily obtain that $P_R(j) = (2\sqrt{\pi})^{-1}\sigma_R(j)$ for $\sigma_R(j) \ll 1$. The probability of the inverse event, namely, $\mathrm{Re}\, f_j' x_j < 1$ and $\mathrm{Re}\, f_j' y_j > 1$, is also equal to $P_R(j)$ due to the symmetry. Similarly, for shifts of imaginary parts, the probability will be $P_I(j) = (2\sqrt{\pi})^{-1}\sigma_I(j)$ where $\sigma_I(j)$ is the standard deviation of $\mathrm{Im}(x_j - y_j)$ (in general it differs from $\sigma_R(j)$). Recalling now that we have N independent maps, we get the full

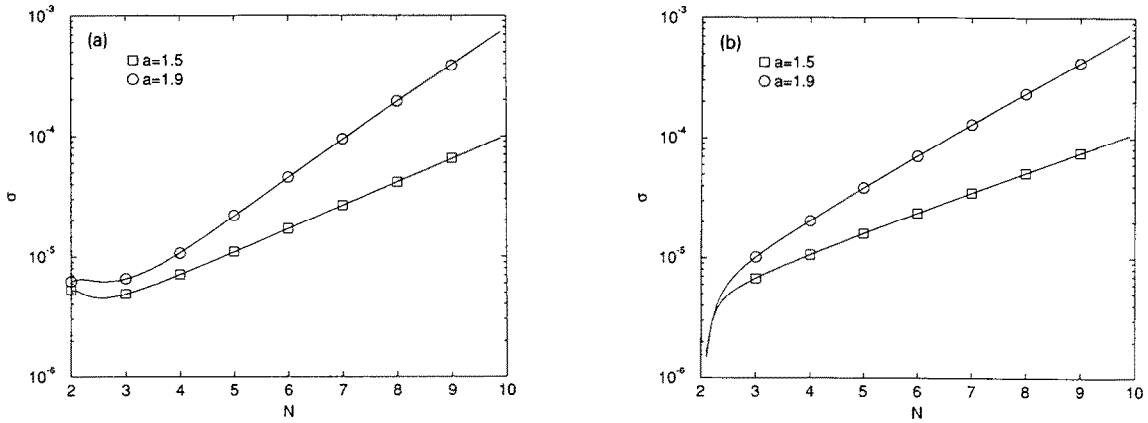

Fig. 6. Standard deviations of $\mathrm{Re}(x_j - y_j)$ (a) and $\mathrm{Re}(x_j - y_j)$ (b) as functions of N for super-stable coupled complex shift maps (14) with $f_0 = 1.5$, 1.9, and white noise magnitude $\sigma = 10^{-5}$.

probability of de-synchronization at a given iteration, $P_N = \sum_{j=1}^{N}[P_R(j) + P_I(j)] = (2\sqrt{\pi})^{-1}\sum_{j=1}^{N}(\sigma_R + \sigma_I)$. The probability of having a break at exactly the lth iteration is evidently $P(l) = (1 - P_N)^{l-1}P_N$. In the limit of $P_N \ll 1$ which corresponds to the situation when the probability of de-synchronization at a particular step is small, this yields the exponential probability distribution (30) with $\Delta \approx (2\sqrt{\pi})^{-1}\sum_{j=1}^{N}[\sigma_R(j) + \sigma_I(j)]$. It remains to express $\sigma_{R,I}(j)$ in terms of the noise standard deviation σ and the number of maps N. It is not difficult to compute these relations analytically taking advantage of the special form of the Jacobian matrix DF. Indeed, the linearized equation for the vector of $\boldsymbol{\xi} \equiv \boldsymbol{x} - \boldsymbol{y}$ reads as

$$\boldsymbol{\xi}(n+1) = \mathsf{DF}\boldsymbol{\xi}(n) + \boldsymbol{\eta}(n), \tag{33}$$

where vector $\boldsymbol{\eta}(n)$ represents noise in the channel. Note that by assumption all N components of the vector $\boldsymbol{\eta}(n)$ are equal. After iterating Eq. (33) $N-1$ times and using nilpotency of DF ($\mathsf{DF}^N = \mathbf{0}$), one obtains

$$\boldsymbol{\xi}(n+N) = \mathsf{DF}^{N-1}\boldsymbol{\eta}(n) + \mathsf{DF}^{N-2}\boldsymbol{\eta}(n+1) + \ldots + \boldsymbol{\eta}(n+N-1). \tag{34}$$

It is easy to see that $[\mathsf{DF}^M\boldsymbol{\eta}(n)]_j = f_j^M\eta(n)$, where η is a component of the vector $\boldsymbol{\eta}$. The standard deviation of the arbitrary component of $\boldsymbol{\xi}$ can be readily found under the assumption that $\eta(n)$ are δ-correlated, $\langle\eta(i)\eta(j)\rangle = \frac{1}{12}\sigma^2\delta_{ij}$. For f_0 real, statistical averaging of the sum (34) yields the following expression for the standard deviation of $\mathrm{Re}\,\xi$, $\mathrm{Im}\,\xi$:

$$\sigma_{R,I}(j) = \sigma\sqrt{\frac{1}{24}\left(f_0^{2N} - 1\right)\left(\frac{1}{f_0^2 - 1} \pm \frac{f_0^2\cos(4\pi j/N) - 1}{f_0^4 - 2f_0^2\cos(4\pi j/N) + 1}\right)}. \tag{35}$$

This formula agrees precisely with numerical simulations (see Fig. 6). The sum of all standard deviations cannot be calculated exactly, but still Δ can be approximated by a simple formula,

$$\Delta = \frac{c\sigma N f_0^N}{\left[48\pi(f_0^2 - 1)\right]^{1/2}}, \tag{36}$$

where c is an O(1) constant. This formula also agrees with our numerical simulations. Fig. 7 illustrates the linear dependence of Δ on σ, and Fig. 8 demonstrates that the $\Delta(N)$ is well fitted by the function (36).

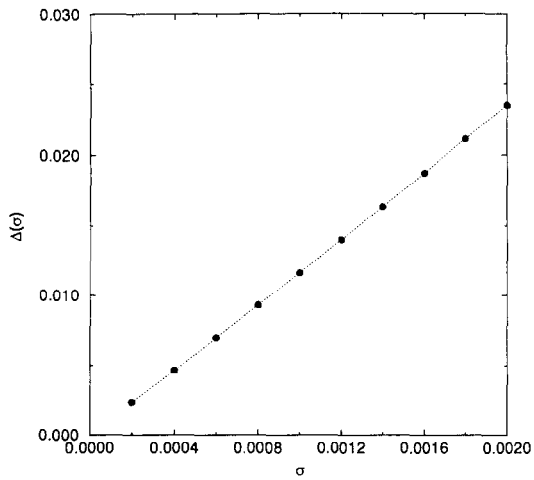

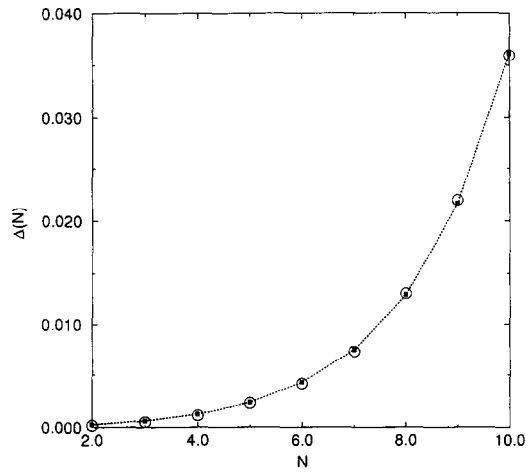

Fig. 7. Rate Δ of exponential decay of the probability distribution $P(l)$ as a function of the noise level σ for $f_0 = 1.5$, $N = 5$.

Fig. 8. Rate Δ of exponential decay of the probability distribution $P(l)$ as a function of the number of map pairs N for $f_0 = 1.5$, $\sigma = 2 \times 10^{-4}$. The open circles correspond to the results of numerical simulations while the dotted line with solid squares shows the fitting of these data with $6.3 \times 10^{-5} N f_0^N$.

3. Continuous systems

So far we have studied multiple synchronization of discrete-time systems (maps). To test our idea of multiple synchronization in the *continuous time* systems, we studied numerically the system of ODEs that simulates the dynamics of the coupled electronic circuits [9]:

Driving system:

$$\dot{x}_1^{(1)} = y_1^{(1)}, \qquad \dot{y}_1^{(1)} = -x_1^{(1)} - \delta_1 y_1^{(1)} + z_1^{(1)}, \qquad \dot{z}_1^{(1)} = \gamma_1 \left[\alpha_1 f\left(x_1^{(1)}\right) - z_1^{(1)}\right] - \sigma_1 y_1^{(1)},$$
$$\dot{x}_1^{(2)} = y_1^{(2)}, \qquad \dot{y}_1^{(2)} = -x_1^{(2)} - \delta_2 y_1^{(2)} + z_1^{(2)}, \qquad \dot{z}_1^{(2)} = \gamma_2 \left[\alpha_2 f\left(x_1^{(2)}\right) - z_1^{(2)}\right] - \sigma_2 y_1^{(2)}, \tag{37}$$

Response system:

$$\dot{x}_2^{(1)} = y_2^{(1)} + \epsilon\left[x_1^{(1)} + x_1^{(2)} - x_2^{(1)} - x_2^{(2)}\right], \qquad \dot{y}_2^{(1)} = -x_2^{(1)} - \delta_1 y_2^{(1)} + z_2^{(1)},$$
$$\dot{z}_2^{(1)} = \gamma_1 \left[\alpha_1 f\left(x_2^{(1)}\right) - z_2^{(1)}\right] - \sigma_1 y_2^{(1)}, \qquad \dot{x}_2^{(2)} = y_2^{(2)} + \epsilon\left[x_1^{(1)} + x_1^{(2)} - x_2^{(1)} - x_2^{(2)}\right],$$
$$\dot{y}_2^{(2)} = -x_2^{(2)} - \delta_2 y_2^{(2)} + z_2^{(2)}, \qquad \dot{z}_2^{(2)} = \gamma_2 \left[\alpha_2 f\left(x_2^{(2)}\right) - z_2^{(2)}\right] - \sigma_2 y_2^{(2)}. \tag{38}$$

In an appropriate parameter range, each driving oscillator behaves chaotically. The meaning of the parameters entering these equations as well as the shape of the nonlinearity $f(\cdot)$ can be found in [9].

In our numerical simulations we used the following values of parameters: $\delta_{1,2} = 0.534$, $\gamma_{1,2} = 0.2$, $\sigma_{1,2} = 1.52$, $\alpha_1 = 22.4$, $\alpha_2 = 23$. We found that this system behaves in a manner similar to the one described in the previous section. In Fig. 9 we show the synchronization error $x_1^{(1)} - x_2^{(1)}$ as a function of time for the case of strong coupling, $\epsilon \to \infty$. The driving and response systems were started from the initial conditions in the manifold of synchronized motions. Eqs. (37), (38) were integrated using an adjustable-stepsize Runge–Kutta method. Once every unit of time, the uniformly distributed white noise of magnitude 2×10^{-5} was added to the dynamical variables of the response system. As in discrete systems, we observed an intermittent behavior.

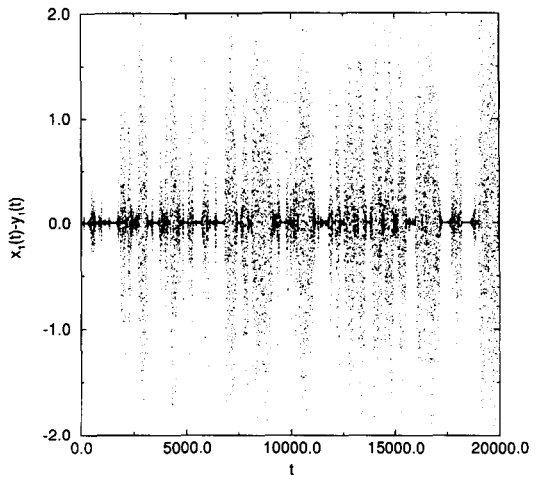

Fig. 9. Typical time series of the difference between driving and response signals $x_1 - y_1$ for two pairs of coupled ODEs (37), (38).

The synchronization persists for some finite time, then breaks due to noise amplification along a piece of trajectory with positive local Lyapunov exponent, and after a while returns to the vicinity of the invariant manifold of synchronized dynamics. The characteristic length of laminar intervals is dramatically affected by the level of noise that we introduced. The important difference between the intermittency in coupled maps and the intermittency in the continuous system (37), (38), is that due to the higher dimensionality of the phase space in the latter case, the transient process that follows the initial outburst is much longer. Once the system abandons the manifold of synchronized oscillations, it may wander around for a very long time before it settles on the manifold again. In practice, some error-correcting scheme can be developed that resets synchronization "manually" right after the de-synchronization burst occurs.

4. Conclusions

In this work we have demonstrated the principal possibility of sending simultaneously several *independent* chaotic signals over one communication channel and separating them at the receiver using the phenomenon of chaotic synchronization. Several examples have been used to illustrate the main ideas, coupled maps as well as ordinary differential equations. The systems at the receiver end are globally coupled and synchronized by a sum of signals generated by uncoupled driving systems at the transmitter end. By the optimal choice of coupling strength and the form of nonlinearity, the manifold of synchronized motion $x = y$ can be made stable (the maximal global conditional multiplier is less than unity, or the maximal global conditional Lyapunov exponent is negative). Moreover, for some particular class of shift maps, *all* multipliers are zero, i.e. the invariant manifold is super-stable.

Unfortunately, despite of superstability, a finite (actually, rather small) amount of noise in the communication channel is able to destroy synchronous behavior of the response systems. The reason for that, as explained in Subsection 2.3, is that local conditional multipliers of the invariant manifold can be larger than unity (in continuous systems local conditional Lyapunov exponents are positive) for relatively long periods of time and therefore amplify noise to the large-scale de-synchronization outbursts or even driving the system beyond the basin of attraction of synchronous dynamics. In the case of shift maps the local multipliers are all zero (see Subsection 2.2), however the shifts themselves may break synchronization if noise is present in the channel. As is typical for so-called "on–off" intermittency, long laminar periods of synchronized behavior are separated

by bursts of complete de-synchronization. We calculated analytically and numerically the distribution function of lengths of laminar phases as a function of the number of systems and the noise level.

From the practical point of view, more sensible would be simultaneous transmission of several information-bearing signals rather than purely chaotic ones. We believe that with some modification, our approach can be used for this purpose. Indeed, in a number of recent publications various methods of controlling chaos have been proposed. In particular, Hayes et al. [3] demonstrated that a chaotic system can be forced to follow a given symbolic sequence by applying very small albeit carefully chosen perturbation to its parameters. Applying this method, one can control all driving systems independently, and thus embed the signals into the chaotic sequences. Note that since the control is small, these sequences do not differ from "uncontrolled" time series from the same systems in a sense that they could be generated by those systems if the initial conditions were appropriately chosen. So, the sum of these signals should synchronize the response systems as well as the sum of "uncontrolled" chaotic signals, and therefore, the multiple information signals can be retrieved.

Acknowledgement

We are grateful to H. Abarbanel, N. Rulkov, and M. Rabinovich for helpful discussions. This work was supported by the U.S. Department of Energy under contract No. DE-FG03-95ER14516 and by the Office of Naval Research under grant No. N00014-92-J-1545.

References

[1] H. Fujisaka and T. Yamada, Progr. Theor. Phys. 69 (1983) 32;
V.S. Afraimovich, N.N. Verichev and M.I. Rabinovich, Radiophys. Quantum Electron. 29 (1986) 795;
H.G. Winful and L. Rahman, Phys. Rev. Lett. 65 (1990) 1575;
N.F. Rulkov and A.R. Volkovskii, Tech. Phys. Lett. 19 97 (1993);
R. Roy and K.S. Thornburg, Phys. Rev. Lett. 72 (1994) 2009.
[2] L.M. Pecora and T.L. Carroll, Phys. Rev. Lett. 64 (1990) 821.
[3] S. Hayes, C. Grebogi and E. Ott, Phys. Rev. Lett. 70 (1993) 3031.
[4] K.M. Cuomo and A.V. Oppenheim, Phys. Rev. Lett. 71 (1993) 65;
A.R. Volkovskii and N.F. Rulkov, Tech. Phys. Lett. 19 (1993) 97;
L. Kocarev et al., Int. J. Bif. and Chaos 3 (1993) 1619.
[5] G.R. Cooper, Modern communications and spread spectrum (McGraw-Hill, New York, 1986).
[6] A.J. Viterbi, CDMA: Principles of spread spectrum communication (Addison-Wesley, Reading, MA, 1995).
[7] V.I. Oseledec, Moscow Math. Soc. 19 (1968) 197.
[8] A.S. Pikovsky, Z. Phys. B 55 (1984) 149;
N. Platt, E.A. Spiegel and C. Tresser, Phys. Rev. Lett. 70 (1993) 279;
E. Ott and J.C. Sommerer, Phys. Lett. A 188 (1994) 39.
[9] N.F. Rulkov, L.S. Tsimring and H.D.I. Abarbanel, Phys. Rev. E 50 (1) (1994) 314.
[10] P. Lancaster and M. Tismenetsky, The theory of matrices, 2nd Ed. (Academic, New York, 1985).
[11] R. Brown, N.F. Rulkov and N.B. Tuffilaro, Phys. Rev. E 50 (1994) 4488;
J. Heagy, T.L. Carroll and L.M. Pecora, Phys. Rev. E 52 (1995) R1253.
[12] J. Theiler, S. Nichols and K. Weisenfeld, Physica D 80 (1995) 206.